TEKNILLINEN TIEDEKUNTA

THERMAL RESISTANCE OF HOT-PRESSED PAPER MILL FLY ASH

Pinja Moilanen

PROCESS ENGINEERING

Bachelor's Thesis

January 2022

TIIVISTELMÄ

Kuumapuristusmenetelmällä valmistetun paperitehtaan lentotuhkan lämmönkesto

Pinja Moilanen

Oulun yliopisto, prosessitekniikan tutkinto-ohjelma

Kandidaatintyö 2022, 31 s.

Työn ohjaaja(t) yliopistolla: Jari Ruuska, Samira Moukannaa

Betoni on yksi käytetyimmistä rakennusmateriaaleista ja sen tärkein raaka-aine, Portland-sementti, on merkittävä kasvihuonepäästöjen aiheuttaja. Sementille on kehitetty lukuisia ympäristöystävällisiä vaihtoehtoja, joista lupaavia ovat alkaaliaktivoidut materiaalit. Niiden raaka-aineina voidaan käyttää erilaisia teollisuuden sivutuotteita, kuten lentotuhkaa ja masuunikuonaa, joita aktivoidaan emäsaktivaattorilla. Tämä edistää kiertotaloutta ja vähentää kasvihuonepäästöjä. Rakennusmateriaalit kohtaavat useita erilaisia haasteita, kuten korroosiota ja korkeita lämpötiloja. Tämän työn tarkoituksena oli tutkia erään alkaaliaktivoidun materiaalin lämmönkestoa. Työssä tutkittiin lentotuhkasta eri metodeilla valmistettujen alkaaliaktivoitujen näytteiden taivutus- ja puristuslujuutta, sekä muutoksia näytteiden kiderakenteessa altistettaessa näytteitä korkeille lämpötiloille. Paperiteollisuuden sivutuotteena syntyvää lentotuhkaa käytettiin pääraaka-aineena ja standardisoitua hiekkaa aggregaattina. Emäsaktivaattorina käytettiin seosta, joka sisälsi natriumsilikaattia, natriumhydroksidia ja deionisoitua vettä. Näytteiden valmistuksessa hyödynnettiin perinteisen kovettamisen lisäksi kuumapuristustekniikkaa. Näytteitä kovetettiin kolmessa eri lämpötilassa: 150 °C, 225 °C ja 300 °C. Tämän jälkeen näytteet asetettiin kovettumaan huoneenlämpöön. Kahden kuukauden jälkeen näytteet altistettiin kolmelle eri lämpötilalle: 500 °C, 800 °C ja 1000 °C. Tulosten perusteella kuumapuristustekniikka on erittäin hyödyllinen tapa valmistaa lentotuhkapohjaisia alkaaliaktivoituja materiaaleja. Näytteet osoittivat hyvää lämmönkestoa ja erityisesti puristuslujuus säilyi hyvin korkeille lämpötiloille altistettaessa. Röntgendiffraktioanalyysi osoitti myös, että näytteiden faasirakenne muuttui ja uusia amorfisia faaseja muodostui.

ABSTRACT

Thermal resistance of hot-pressed paper mill fly ash

Pinja Moilanen

University of Oulu, Process Engineering

Bachelor's thesis 2022, 31 pp.

Supervisor(s) at the university: Jari Ruuska, Samira Moukannaa

Concrete is one of the most common construction materials, and its main raw material, Ordinary Portland Cement (OPC), is a significant greenhouse emitter. Numerous environmentally friendly alternatives have been developed for cement, from which alkali-activated materials (AAMs) are promising ones. Various industrial by-products such as fly ash (FA) and blast furnace slag (BFS) can be used as raw materials, and they are activated using an alkaline activator. This promotes the circular economy and reduces greenhouse emissions. Construction materials face different challenges, including corrosion and high temperatures. This work aimed to study the heat resistance of one of the AAMs. The work studied the flexural and compressive strengths of samples made from FA using various methods, as well as the changes in the crystal structure of the samples when they are exposed to high temperatures. FA from a by-product of the paper industry was used as raw material and standardized sand as an aggregate. A mixture containing sodium silicate, sodium hydroxide, and deionized water was used as an alkaline activator. In addition to conventional curing, a hot-pressing technique was utilized to prepare samples. Samples were cured at three different temperatures: 150°C, 225°C, and 300°C. Afterward, the samples were set to cure at room temperature. After two months, the samples were exposed to three different temperatures: 500°C, 800°C, and 1000°C. Based on the results, the hot-pressing technique is useful for preparing FA-based AAMs. The samples showed good heat resistance and especially, compressive strength remained when they were exposed to high temperatures. X-ray diffraction analysis (XRD) also showed that the phase structure of the samples was changed, and new amorphous phases were formed.

TABLE OF CONTENTS

TIIVISTELMÄ
ABSTRACT
TABLE OF CONTENTS
LIST OF SYMBOLS AND ABBREVIATIONS
1 INTRODUCTION 7
2 ALKALI-ACTIVATED MATERIALS 9
2.1 AAMs in construction materials 10
2.2 Pulp and paper mill fly ash 12
2.3 Fire resistance of AAMs 13
2.4 Hot pressing 14
3 MATERIALS AND METHODS 16
3.1 Raw materials 16
3.2 Sample preparation 17
3.3 Thermal treatment 17
3.4 Analysis methods 20
3.4.1 X-ray diffraction 20
3.4.2 Flexural strength 20
3.4.3 Compressive strength 21
4 RESULTS AND DISCUSSION 22
4.1 X-ray diffraction 23
4.2 Flexural strength 24
4.3 Compressive strength 26
5 CONCLUSIONS 29
REFERENCES

LIST OF SYMBOLS AND ABBREVIATIONS

σ_C	Compressive strength
σ_F	Flexural strength
F	Maximum compressive/flexural load
L	Span length
AAC	Alkali activated cement
AAM	Alkali activated material
BFS	Blast furnace slag
FA	Fly ash
GPC	Geopolymer cement
OPC	Ordinary Portland Cement
PMA	Paper mill ash
PPFA	Pulp and paper mill fly ash
XRD	X-ray diffraction

.

1 INTRODUCTION

The world's enormous consumption has led to a growing need for raw materials processed into products in various industrial processes. However, in addition to the intended products, a significant number of by-products also is being generated in industrial processes. Their formation causes challenges, as they usually are unexploited. Pulp and paper mill fly ash (PPFA) is a by-product of the pulp and paper industry which amount is growing fast due to the increasing demand for different paper applications. Generally, PPFA is treated as non-hazardous commercial waste and used as a landfill. However, the upcoming regulations concerning landfilling force to develop the alternatives. Instead of landfilling, new ways have been developed to utilize the ash by recycling and reusing it. One of the applications is the valorization of the ash to alkali-activated materials (AAMs), which are treated as an environmentally friendly alternative to Ordinary Portland cement (OPC) in construction materials (Cherian & Siddiqua, 2019).

AAMs are inorganic polymers, and they are generated by the alkali activation reaction between raw material and an alkaline activator. Construction materials have many requirements for durability and resistance in aggressive environments so it's vital to study the properties of AAMs. Alkali-activated cements (AACs) have been studied to have comparable or superior properties compared to OPC in mechanical properties, durability, and resistance in an aggressive environment such as high temperature or conditions with low pH. Additionally, the production of AACs is much more sustainable, and it produces less CO_2 emissions compared to OPC (Provis & van Denventer, 2013, p.12). There are several ways to enhance the properties of AAMs: the pre-treatment of the raw materials, including grinding, the addition of other reactive precursors, thermal treatment, and curing conditions (Pacheco-Torgal et al., 2008).

MIMEPRO is a project funded by Business Finland that aims to advance the circular economy in terms of zero waste, reduced use of raw materials, and reusing and recycling of materials. The project is coordinated by the University of Oulu and its main purpose is to utilize the inorganic industrial waste and side streams instead of landfilling. This study aims to research the thermal resistance of hot-pressed PPFA. Although there are many studies of AAMs and their properties, studies about alkali activation of different raw materials are needed so that different industrial side streams could be utilized as widely as possible. It is also essential to study different methods to enhance the properties of

AAMs. The hot-pressing curing method was recently presented as an efficient way to enhance the properties of inorganic polymers by reducing pore size and porosity (Ranjbar et al., 2020).

This thesis consists of the following parts: Chapter 2 gives detailed information on AAMs and their properties. The used materials and methods are introduced in Chapter 3. The compressive and flexural strength tests were made to the samples alongside the X-ray diffraction (XRD) to determine the changes in the mechanical properties and microstructure of the samples. The results are presented and discussed in Chapter 4. In Chapter 5 the most important study information is brought together.

2 ALKALI-ACTIVATED MATERIALS

AAMs are widely considered as a family of alternative binders to OPC due to their promising engineering and environmentally friendly properties. Theoretically, any binder system based on the reaction between an alkali metal source and a solid aluminosilicate powder can be classified as AAM. The alkali sources are also known as activators, and they can be solid or dissolved and include different alkali compounds. Usually, metal hydroxides or soluble silicates are used as activators in alkali activation reactions. The solid, also called raw material, can be a calcium silicate or a more aluminosilicate-rich material (Provis & van Denventer, 2013, p.7). Secondary raw materials from industries are mainly used as raw materials (Singh & Middendorf, 2020). The reaction mechanism between the alkali activator and the raw material is based on a three-step model of dissolution, orientation, and hardening. Both the reaction mechanism and the reaction products depend on the alkali activator and the raw materials. In calcium-rich systems, the main reaction product is amorphous calcium silicate hydrate gel (C-S-H). When a higher amount of aluminum is present, the main reaction product is more zeolite-like polymers. The word “geopolymer” was first proposed by French researcher Joseph Davidovits in 1978. He developed and patented multiple aluminosilicate-based binders (Pacheco-Torgal et al., 2007). Geopolymers are considered a subset of AAMs with a high amount of aluminosilicate binding phase and a relatively low amount of calcium content. Figure 1 shows the classification of different binder groups. The binders are placed on a three-dimensional coordinate system and the axis are demonstrating the chemical contents of different raw materials. The chemical contents are increasing Ca content, increasing Al content, and increasing M+ content where M describes the alkaline metal ion (Na and/or K) content (Provis & van Denventer, 2013, p.8). The alkali activation process of geopolymers is also called geopolymerization.

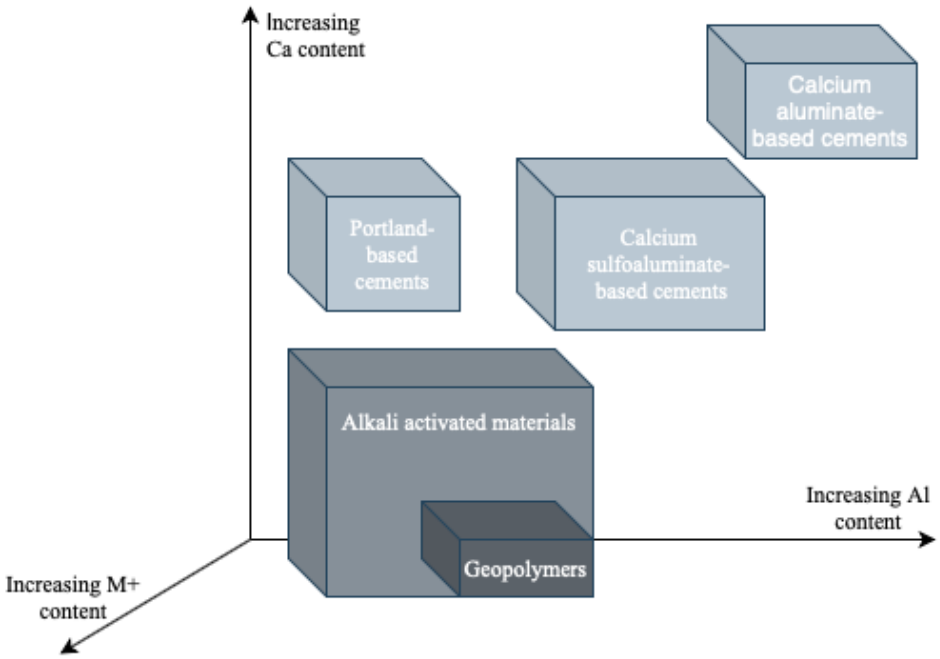

Figure 1. Classification of AAMs, with comparison to other common binders (retell Provis & van Denventer, 2013, p.8).

The amorphous phases are the most reactive components in the raw materials and the efficiency of alkali activation is highly dependent on the total amorphous phase content. The more amorphous phase, the more efficient and easier is the gel formation (Christelo, 2016). This has a positive effect on the mechanical properties of the alkali-activated materials. For example, the compressive strength improves while the amorphous phase content in the raw material increases. The most common raw materials used in alkali activation applications are fly ash (FA), metakaolin (MK), and blast furnace slag (BFS). Besides them, the other reactive and amorphous or semi-crystalline silicate materials have been proven to be exploitable as well (Scrivener et al., 2018, p.16). Those are, for example, metallurgical slags, calcined clays, kaolin, and red mud.

2.1 AAMs in construction materials

Concrete is one of the world's most common construction materials. Alkali-activated cements (AACs) including geopolymer cements (GPCs) are considered a sustainable alternative to OPC, the main binding material of concrete. About 4 billion tons of OPC is produced annually and the CO_2 emissions of OPC concern 5-7 % of the world's CO_2 emissions (Singh & Middendof, 2020). In addition to CO_2, the other greenhouse gases

are emitted as well during cement production. Altogether it is estimated that greenhouse gas emissions of OPC are about 1.5 billion tons annually, which is 7-8 % of all the greenhouse emissions in the world (Singh & Middendof, 2020).

The structural performance of AACs is studied to be equivalent or superior to OPC. Because of their ambient curing conditions, they can be utilized in many stages of construction. In many studies. compressive strengths from 50 MPa to 110 MPa have been reported both for the BFS high-calcium binder systems and FA-based low-calcium binder systems The mix design along with the optimized aggregate content and appropriate liquid to binder -ratios can provide AACs suitable for many structural applications. (Mangat & Lambert, 2016). GPC has been studied to have comparable or even better mechanical properties than OPC. For example, GPC has higher early strength and similar or better durability compared to OPC (2020 Amran). Figure 2 shows the basic performance differences between OPC concrete and GPC. It presents that GPC has superior properties to OPC especially when it comes to durability, formability, and sustainability.

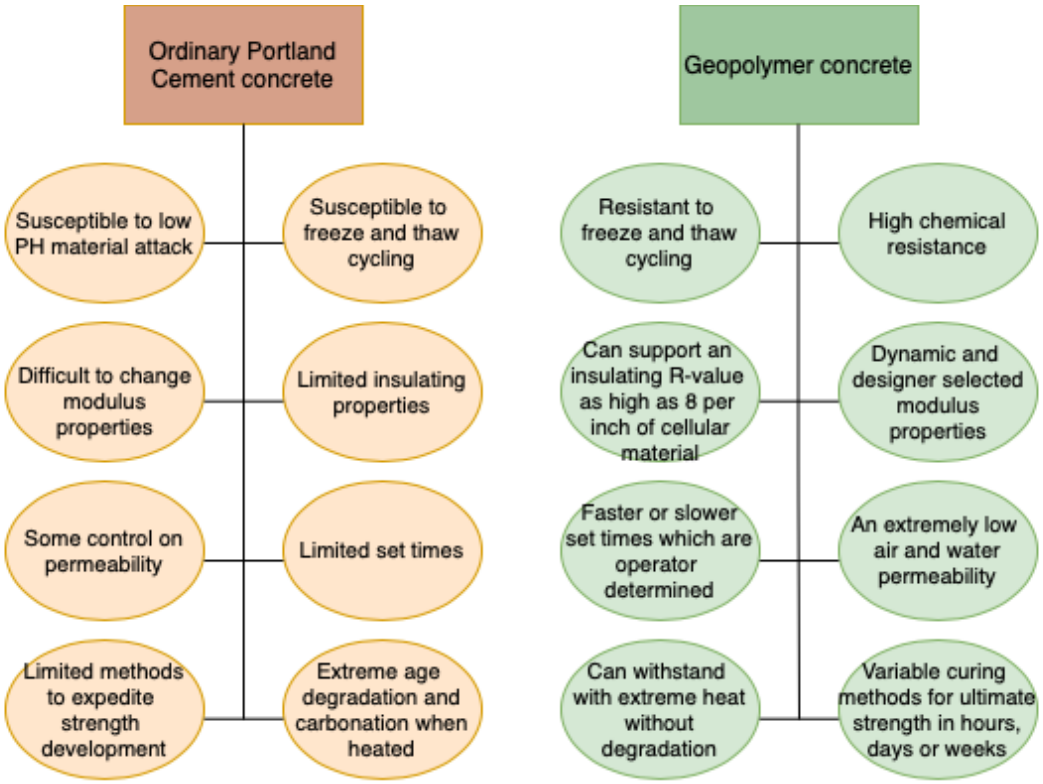

Figure 2. Comparison between the performance of OPC concrete and GPC (retell Hassan et al., 2019).

An alkali-activated FA, a by-product of coal combustion in thermal power plants, was studied. By activating FA using a mixture of NaOH pellets and sodium silicate, a cementitious material with high mechanical strength (more than 35 MPa cured at 85 °C for 2 h) was produced as a reaction product (Palomo et al., 1999). Subsequently, there have been published many studies concerning FA. It has become one of the most utilized raw materials in alkali-activated construction applications. Considering the low cost, low CO_2 emissions and low energy usage in the production of the FA-based geopolymer, the FA cement and concrete has been considered as a great alternative to OPC. Additionally, the alkali activation process can trap toxic metal elements from FA (Zhuang et al., 2016). The applications for low-Ca AAMs can be generally divided into two different fields: the materials can be used as a cement-like binder and a low-cost alternative for burnt ceramics (Provis & van Denventer, p. 95). Besides the FA-based cements and concretes, FA-based AAMs have been used in different applications including material manufacturing (glass ceramics and bricks), pavement construction, as a fill material for the embankment construction, and road construction (Cherian & Siddiqua, 2019).

Coal FA can be divided into Class F ash which contains less than 10 % calcium oxide and Class C ash where the Ca content is more than 10 % (Wardhono, 2018). Especially Class F ash is widely used in AAMs. In addition to a coal FA, which is produced from the burning of pulverized coal in a boiler the other types of ashes are utilized in AAM technology. Bottom ash is also obtained from coal-fired boilers and it's much coarser than FA (Provis & van Denventer, 2013, p. 82). Biomass ash is a residual from a biomass thermal power plant. The characteristics of biomass ashes are highly dependent on the biomass used. Biomass can be an agricultural waste, herbaceous biomass, wood, or bark (Rajamma et. al., 2009). The other common type, PPFA, is discussed below.

2.2 Pulp and paper mill fly ash

PPFA is a non-hazardous waste product of the pulp and paper industry which is known for its suitable properties for sustainable development. Because of its high calcium aluminosilicate and calcium concentrations, it has self-cementation properties which makes it exploitable to many promising fields such as the construction industry or soil stabilization. PPFA is very light, and its other characteristics are particle fineness, the irregularity of particle sizes, and its porous nature. PPFA's density decreases as the carbon content increases. The average particle size variates between 150 and 250 μm. PPFA can

include different concentrations of trace metals which are categorized as hazardous to human health (Cherian & Siddiqua, 2019).

The goal of valorization of PPFA is to transform potentially hazardous residuals into stable AAMs (Cherian & Siddiqua, 2019). In 1999 Hackett et al. studied the composting of PPFA with wastewater treatment sludge. As a product, they got an acceptable soil conditioner with many essential nutrients for plant growth and liming ability. In 2011 Mohammed & Fang investigated the use of paper-mill residuals in concrete formulations to obtain an alternative to landfill disposal. Even if the paper-mill residuals content decreased the mechanical and the durability properties of mixtures, the concrete mixtures with Class F FA improved the resistance to chloride-ion penetration and surface permeation. PPFA waste has also been used for brick making. Sarkar et al. (2017) Lime mud, which was obtained from PPFA was used in the brickmaking as a replacement of natural soil.

Different parameters can enhance the properties and improve the alkali activation reaction of the FA and PPFA. Those are, for example, the pre-treatment of the raw materials, the quantity of the activator, and the curing conditions, especially the temperature. According to Fan et al. (2017), the residual strength of FA-based geopolymers reached up to 96 MPa as the compressive strength reached more than 100 MPa after heating the samples at 500 °C. Recently, hot pressing was introduced as a method to accelerate the kinetics of the alkali activation and enhance the properties of the AAMs (Ranjbar et al., 2020).

2.3 Fire resistance of AAMs

Geopolymer-based concretes are widely used for special construction applications where the performance requirements such as resistance to high temperatures along with fire resistance may be required (Provis & van Denventer, 2013, p. 18). Different tests are done to verify the suitability of the designed AAMs and their resistance to high temperatures. Superior mechanical strength retention after fire exposure and a significantly reduced spalling are the advantages of AAMs over OPC in high-temperature applications. Those applications include tunnel linings, high-rise buildings, lift doors, and marine structures. The structures can either be protected by a fire-resistant coating or they might be built entirely from fire-resistant concrete (Provis & van Denventer, 2013, p. 347).

According to Barbosa et al. (2003), inorganic sodium polysialate geopolymers are thermally stable up to high temperatures. Kaolinite was used as raw material in the study and a variety of inorganic fillers were added to the material. The samples started to melt at about 1300 °C. Zhang et al. (2014) studied metakaolin-fly ash-based (MK-FA) geopolymers for fire-resistant applications and it was shown that MK-FA-based geopolymers have comparable bending and compressive strength as the OPC. Geopolymer paste had a remarkably higher bending strength than the one of OPC paste. Thus MK-FA-based geopolymers can provide comparable or even better fire resistance in structural applications than OPC. Additionally, geopolymers provide many environmental benefits like lower energy consumption and lower CO_2 production during the production of them.

The high-temperature resistance of the FA-based low-calcium binders is superior compared to OPC. Normally while exposed to fire, that internal pressure leads to spalling of OPC concrete. The amorphous gel structure of AAMs provides fire resistance by preventing the formation of internal pressure (Mangat & Lambert, 2016). Kong et al. (2007) compared the performance of MK and FA-based geopolymers while exposed to elevated temperatures. The FA-based geopolymers gained strength while the MK-based ones suffered strength loss after the temperature exposure. FA-based geopolymers had less moisture to escape from FA-matrix and the higher rate of water loss in the MK-based geopolymer was believed to be one of the causes for the strength loss after elevated temperatures. Additionally, He et. al (2020) confirmed in their study that the FA-based geopolymers exhibit good thermal stability at high temperatures.

2.4 Hot pressing

Simultaneous heating and a pressing technique called hot pressing is a way to produce high-strength binders in an extremely short time. It can be viewed as a more efficient way of producing geopolymers as it accelerates the geopolymerization kinetics of the process and reduces the porosity of a geopolymer matrix (Ranjbar et al., 2018). Hot pressing reduces trapped air, which makes the geopolymer structure more compact. Both the reduction in porosity and pore size leads to improved mechanical properties, like an ultra-high early compressive strength. In the study, the porosity reduced to less than 15 wt% when the volcanic ash-based geopolymer samples were hot-pressed at 400 °C with 73.2

MPa. The highest compressive strength accomplished in the study was 160 MPa (Ranjbar et al., 2020).

The schematic mechanism of geopolymerization in hot pressing is shown in Figure 3. In part b) the applied pressure causes the denser structure of the sample through the air removal. After applying the heat in part c), the FA starts to react, and together with pressure, heat, and time in the parts d) to e), the geopolymer gel is formed. Eventually, the sample is cooled in part f) and the final geopolymer sample is formed with a specific volume.

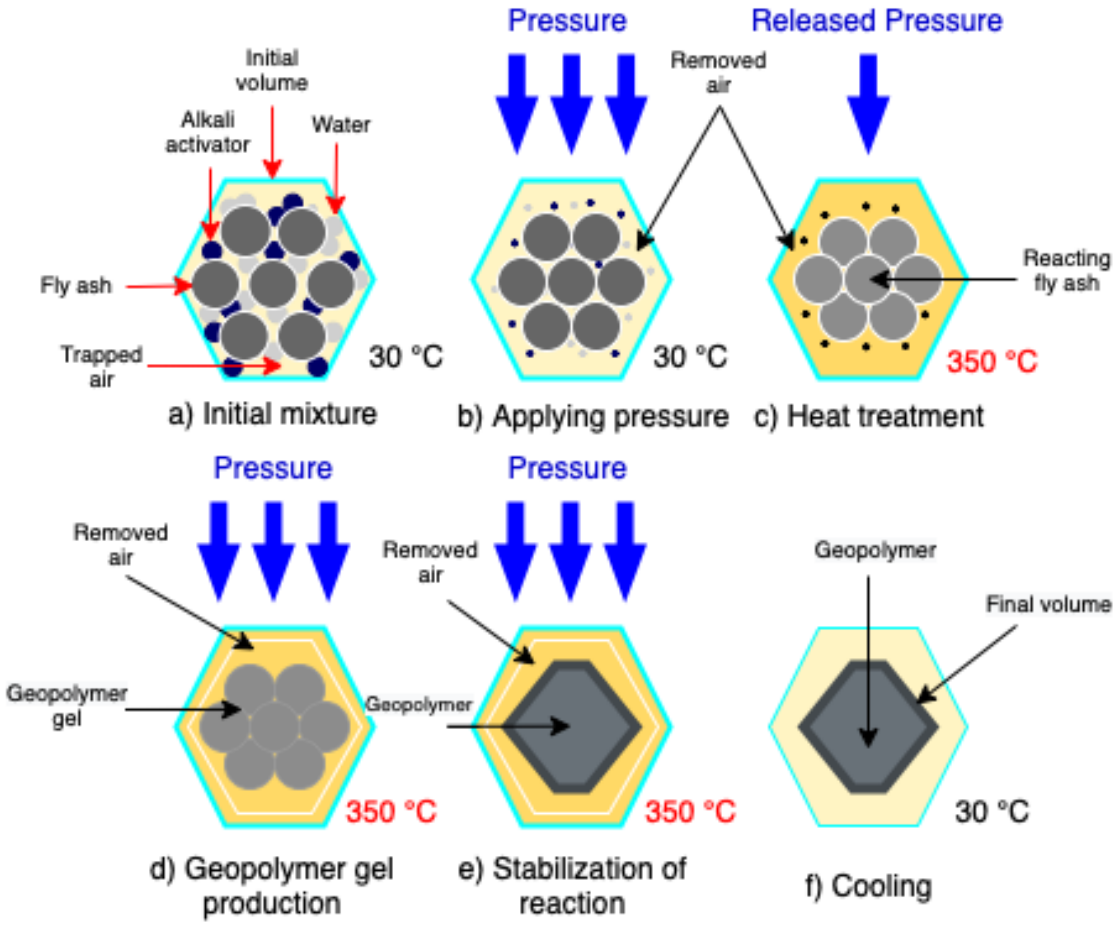

Figure 3. Schematic mechanism of geopolymerization in hot pressing (retell Ranjbar et al., 2017).

3 MATERIALS AND METHODS

3.1 Raw materials

Paper mill ash (PMA) was collected from the electrostatic precipitator (ESP) of paper sludge and paper waste incineration process. The fuel mixture typically combusted in this paper sludge case is 50 % of paper sludge and 50 % of paper wastes with corresponding energy shares of approximately 75 wt% and 25 wt%, respectively. Standard sand was sieved using a 0.7 mm diameter sieve and used as aggregate. Analytical grade NaOH pellets (VWR, Chemicals, Germany) of ≥ 99% purity and Sodium silicate solution (BETOL 50T) containing 31.8% of SiO_2, 12.7% of Na_2O, and 55.5% of H_2O were used as alkali activators. Both mortars with sand and pastes without sand were prepared to make all the tests. NaOH/sodium silicate was selected to achieve a silica modulus of 1 which represents the $sSiO_2/Al_2O_3$ ratio. The mixes composition designs for mortars and pastes are shown in Table 1 and Table 2.

Table 1. Mix composition design of mortars for the hot press.

Mixture (mortar)	Aggregate to ash	NaOH/ Sodium silicate	Activator /binder	Additional water/ binder	Temperature (°C)	Pressure (MPa)	Time (min)
1	0.5	4.08	0.5	0.05	150	130	30
2	0.5	4.08	0.5	0.05	150	130	30
3	0.5	4.08	0.5	0.05	150	130	30

Table 2. Mix composition design of pastes for the hot press.

Mixture (mortar)	Aggregate to ash	NaOH/ Sodium silicate	Activator /binder	Additional water/ binder	Temperature (°C)	Pressure (MPa)	Time (min)
1	0	4.08	0.5	0.05	150	130	30
2	0	4.08	0.5	0.05	150	130	30
3	0	4.08	0.5	0.05	150	130	30

3.2 Sample preparation

The dry components (ESP ash and sieved sand) were mixed in a Kenwood mixer for one minute at a low speed. The deionized water and alkali activator including sodium silicate and NaOH were both weighed on the digital scale and mixed. The formed liquid was added to the dry mixture and mixed for two more minutes at high speed. The pastes were made as described above, but no sand was added.

The prepared mixture was poured into the oiled steel mold with eight slots. Filling occurred gradually in three steps to ensure the homogeneous and dense structure. The mixture was added to the slots and pressed with the steel part in three turns until all the slots are filled. Prepared mold was placed in the hot press machine and pressed. The used temperature, pressure, and time are shown in table 1. The following temperatures were used to prepare three sets of samples: 150 °C, 225 °C, and 300 °C. The pressure and time were constant with each set. The following procedure was also used to form paste-based samples.

After 30 minutes the mold was taken out of the press to cool down. The demolded samples were put in a container and stored at ambient temperature until the high-temperature tests. In addition, a set of reference samples was made to compare the mechanical properties of hot-pressed and normal oven-cured samples at 60 °C.

3.3 Thermal treatment

After two months from the sample preparation, the hot-pressed samples were heated at various temperatures in a high-temperature oven. Every sample group was named separately according to their hot-pressing temperature: HP 1 for 150 °C, HP 2 for 225 °C, and HP3 for 300 °C. The temperatures used in thermal treatment were 500 °C, 800 °C, and 1000 °C. The heating rate was adjusted to 5 degrees/minute. Figure 4 presents a schematic procedure of all the samples prepared in the thesis for different analysis methods from hot pressing to thermal treatment. First, both the mortars and pastes were prepared with a hot press machine using the three different temperatures. Then, they were thermally treated in three different temperatures. Mortar samples were used in

compressive and flexural strength tests, while the XRD measurements were performed for paste samples. Reference samples were prepared to compare between hot-pressing and oven-curing.

The dimensions and weights of the samples were measured before and after exposing the samples to elevated temperatures to determine the possible changes in volume and weight. It is common knowledge that shrinkage appears as a decrease in sample volume, as well as an increase in sample volume, suggests expansion in high temperatures. The change in mass, on the other hand, tells the evaporation or binding of the liquid. Two samples per one hot press temperature were thermally treated in the oven at one temperature. Figure 5 shows the arrangement of the samples in the high-temperature oven.

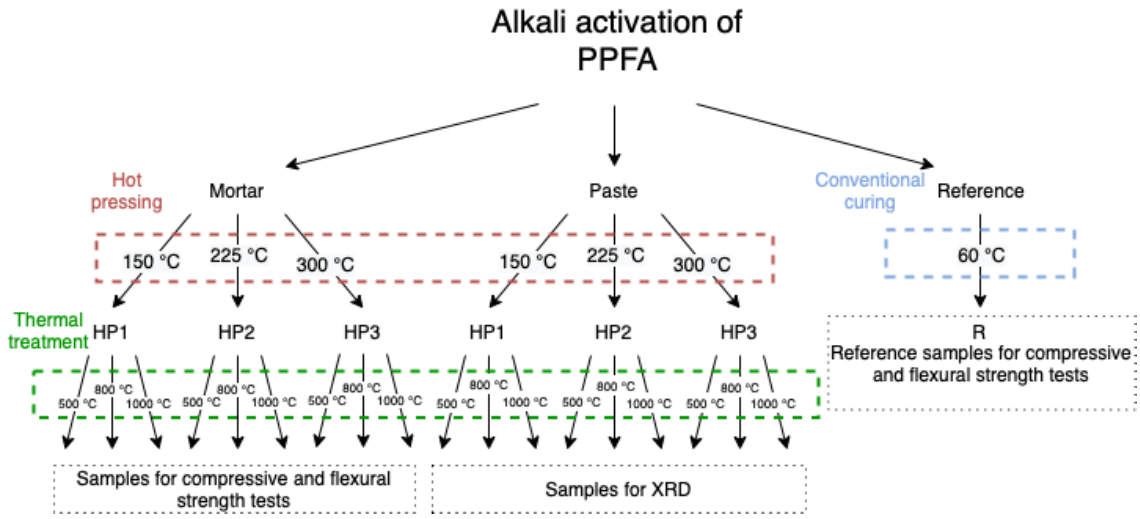

Figure 4. Schematic procedure of samples used for different analysis methods.

Figure 5. Samples in the high-temperature oven.

3.4 Analysis methods

3.4.1 X-ray diffraction

X-ray diffraction (XRD) is a technique used to determine the crystallographic structure of a material. It is based on the monochromatic and high-energy electromagnetic rays, X-rays. In laboratory equipment used sealed tubes and rotating anodes produce X-rays by the same principle. Electrons are generated by heating a tungsten filament in a vacuum and accelerated through a high potential field. After that, they are directed to the target, which emits X-rays. The electrons cause two effects that lead to the generation of X-rays: the deceleration of the electrons leading to the emission of X-ray photons and the ionization of the impinged atoms by ejecting electrons from the inner shells (Epp, 2016). XRD works by irradiating a material with incident X-rays and then measuring the intensities and scattering angles of the X-rays which leave the material. The information is used to phase identification.

3.4.2 Flexural strength

Flexural strength is defined by the maximum stress of a material before it yields. It is measured with a three-point-bending test. The sample was placed with the face that had been cast against the steel of the mold into the device at the center of the supportive rollers and the load was applied continuously until the sample fractured in two parts. Two flexural strength tests were made for each sample. The average of the received two results and the standard deviations were both calculated. Equation 1 below was used to define the flexural strength for each sample:

$$\sigma_F = \frac{3FL}{2b\,d^2}, \tag{1}$$

where σ_F is flexural strength in MPa,
F is maximum flexural load in N,
L is the distance between support rollers in mm,
b is the width of the sample in mm and
d is the depth of the sample in mm.

3.4.3 Compressive strength

A compressive strength test is a method to define the strength of the sample under a compressive load. All the compressive strength measurements were performed at the different ends of the same sample that had first fractured in flexural strength measurements. The sample was placed into the device between the two platens and centered. The load was applied continuously until the sample fractured. Four compressive strength tests were made for each sample, two applying the force on the top side and two applying the force on the lateral surface of the sample. In general, the compressive strength on such prismatic samples is performed using a square metallic plate to simulate cubic dimensions. However, the samples used in the present study have different dimensions than the regular prisms of 20*20*80 mm^3 hence the tests were measured on two sides to check which one is giving accurate results. The samples will be compared with the reference sample tested with a similar method and not with previous results from literature with cubic dimensions. The maximum load in newtons (N) applied to the sample and the cross-sectional area of the bearing plate in millimeters (mm) were used to calculate the compressive strength. It was observed that the samples with applied force on the top side of the sample were giving accurate values. The results were obtained from the average of those two tested samples. Additionally, the standard deviations were calculated for each result. Equation 2 below was used to define the compressive strength for each sample:

$$\sigma_c = \frac{F}{A}, \tag{2}$$

where σ_c is compressive strength in MPa,

F is maximum compressive load in N and

A is a cross-sectional area where the load is asserted in mm^2.

4 RESULTS AND DISCUSSION

The surfaces of the hot-pressed samples in 150 °C before and after thermal treatments after exposure to elevated temperatures are shown in Figure 6. On the left, for comparison, the sample before thermal treatment. The changes in color and surface structure can be observed. The measurements showed that all the samples revealed an average shrinkage of 1.1 % in 500 °C and an average expansion of 7,5 % after the treatment in 800 °C while at 1000 °C the sample fused, and the sand particles were embedded in the paste. They were uncovered while the sample shrunk. Similar changes were observed from the hot-pressed samples at 225 °C and 300 °C.

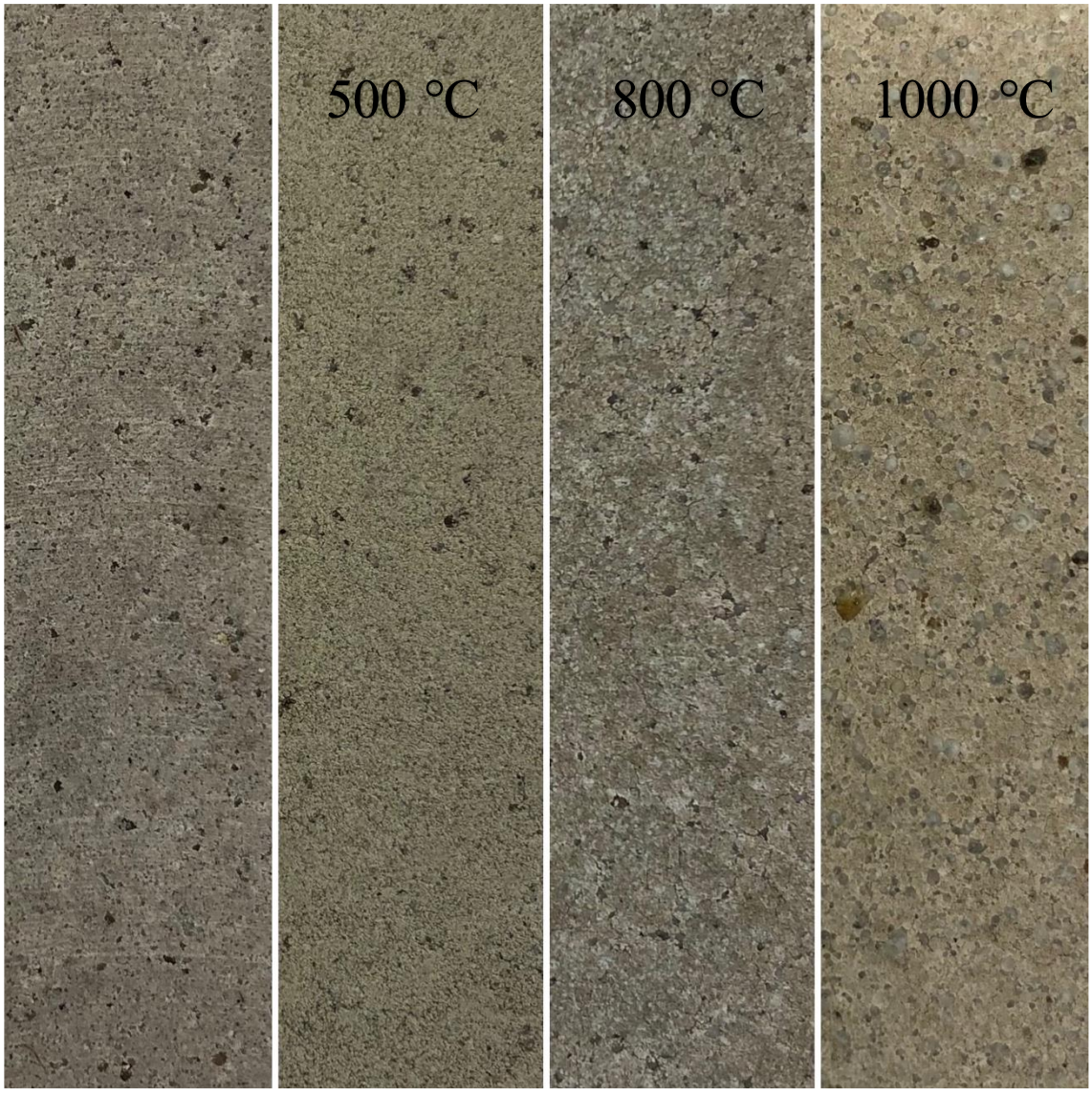

Figure 6. The surfaces of the samples before and after the thermal treatments using different temperatures.

4.1 X-ray diffraction

The XRD patterns of alkali-activated PMA cured using the conventional curing method at 60 ℃ and hot-pressed PMA non-treated and treated in different temperatures are presented in figure 7 alongside the XRD pattern of the raw PMA. Changes in mineralogical composition can be observed in PMA due to alkali activation at high temperatures and pressure. When cured at 60 ℃, portlandite was decomposed from lime. The partial decomposition occurred in the main original phases of PMA which are calcite, gehlenite, and calcium silicate. The hump between 25 and 45 indicates the formation of amorphous reaction products and it is more pronounced to alkali-activated samples. Calcite participates in the formation of amorphous C-S-H gel (Firdous et al., 2021). Sodium carbonate was also formed which indicates the reaction of Na^+ with environmental CO_2 (Firdous & Stephan, 2021). Quartz characteristic peak was also increased which could indicate the partial decomposition of other crystalline phases.

Similar XRD patterns were presented to hot-pressed samples. Some phases such as gehlenite, lime, and calcium silicate were partially decomposed. When treated at 500 ℃, a new phase called sodium aluminum silicate hydrate was formed. This agrees with Moukannaa et al.'s (2019) findings where Na-rich sodium aluminum silicate hydrate was formed at 550 ℃. Some new phases like brearleyite and hydrarogarnet were formed at 800 ℃. For all the samples a disappearance of lime and calcite phases could be explained by their participation in the alkali activation reaction and the formation of the amorphous phases. Additionally, some unknown phases could not identify, especially at 1000 ℃.

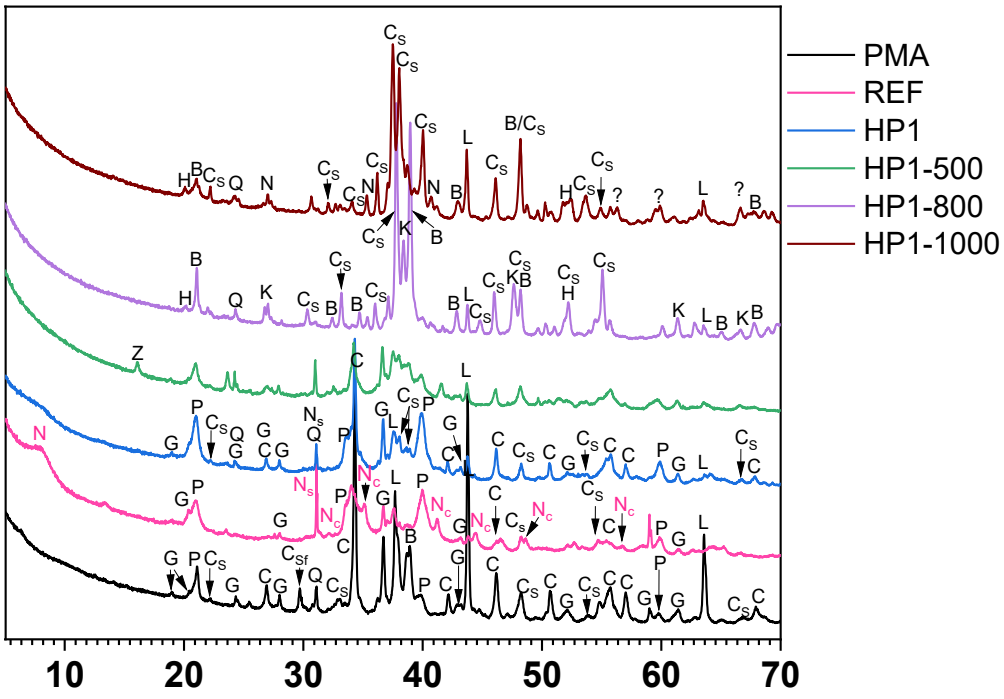

Figure 7. XRD patterns of the raw ash (PMA), the reference sample (REF), the hot-pressed ash non-treated and treated at different temperatures. C: calcite, G: gehlenite; P: portlandite; C_S: calcium silicate; L: lime; Q: quartz; C_{Sf}: calcium sulfate; B: brearleyite; N: natrite; N_S: sodium silicate hydrate; N_C: sodium carbonate; Z: sodium aluminum silicate hydrate; H: hydrarogarnet; K: katoite;?: unknown phases.

4.2 Flexural strength

The average flexural strength test results for each sample are listed in Table 3. Equation 1 was used to calculate the flexural strength. The averages and standard deviations were calculated based on two separate results per sample. The values for the reference sample show the importance of hot pressing. Compared with the conventional curing technique, hot pressing gives a huge advantage on flexural strength.

Figure 7 presents the flexural strength results as a function of heating temperature. It can be noticed that exposure of the samples to elevated temperatures has a negative effect on their flexural strengths. All the exposed samples revealed lower flexural strengths in comparison with the non-treated samples at 25 °C. Flexural strength reaches its lowest value at 500 °C and the value starts to increase again after 500 °C until it reaches 800 °C. A small decrease is noticeable between 800 °C and 1000 °C. In relation, the values vary most in HP2 while for the HP1 and HP3 the variation is lower.

Table 3. Flexural strength test results and standard deviations.

	FLEXURAL STRENGTH			
Temperature	Reference	HP1	HP2	HP3
25	0.89 ± 0.06	6.75 ± 0.360	9.67 ± 1.545	6.34 ± 0.169
500		3.108 ± 0.0236	2.032 ± 0.107	2.683 ± 0.439
800		5.021 ± 0.240	4.041 ± 0.731	4.389 ± 0.074
1000		3.775 ± 1.687	3.360 ± 1.209	2.526 ± 0.0991

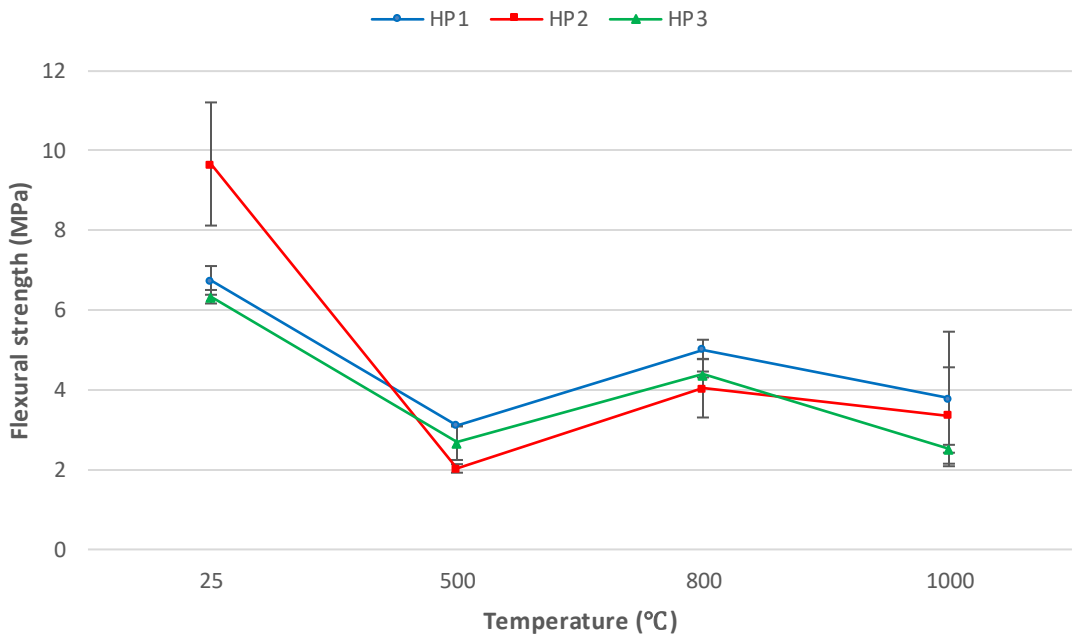

Figure 8. Flexural strength as a function of heating temperature. Error bars represent standard deviations of each result.

According to a study of thermal behavior and mechanical properties of geopolymer mortar after exposure to elevated temperatures by Zhang et al. (2016), the flexural strength of the samples slightly increased at 100 °C, followed by a decrease between 300 and 700 °C. In another study, Mehmet et al. (2018) studied the behavior of geopolymer mortars after exposure to elevated temperatures. The class F FA was used in the study and the mortars were prepared using different curing temperatures. The samples which were cured at ≥ 60 °C started to lose their flexural strength immediately while exposed

to elevated temperatures and the strength decrease occurred till 600 °C. A small increase in strength was observed between 600 and 800 °C. For the samples cured at 50 °C, the flexural strength increased until heating at 200 °C and decreased between 200 and 600 °C. A small increase was also observed between 600 and 800 °C. It was studied that the samples cured in lower temperatures showed more resistance to high temperatures than the samples cured in higher temperatures.

The results achieved in this thesis compared to the above-mentioned studies have some similarities. The flexural strength loss occurs between 25 and 600 °C. Additionally, the samples gain strength between 500 and 800 °C. After being exposed to 1000 °C, the flexural strength decreases slightly. A slight increase could indicate the activation of unreacted PPFA-particles present in samples.

HP1 shows more resistance to high temperatures than HP2 and HP3. It is possible due to the lower curing temperature, which prevents the alkali activation reaction from happening completely while the sample preparation, and at the same time, it enables the complete activation while exposed to higher temperatures (Mehmet et al., 2018). Although, it is unclear why the difference between the flexural strength results of HP2 and HP3 are so significant.

4.3 Compressive strength

The average compressive strength test results are listed in Table 4. Equation 2 was used to calculate the compressive strength. The averages, as well as standard deviations, were calculated based on two separate results per sample. The compressive strength is considerably higher for the hot-pressed samples. The method gives a huge advantage on compressive strength compared to the conventional curing technique.

Figure 8 presents the compressive strength results as a function of heating temperature. For all the samples, the exposure to elevated temperatures induces a decrease in the compressive strengths of the samples. HP1 reaches its lowest value at 800 °C while the values of HP2 and HP3 continue to decrease until they reach their lowest points at 1000 °C. It is noticeable, that even if the initial strength of HP1 is comparatively low, the compressive strength manages well in elevated temperatures. The decrease in compressive strength after high-temperature exposure is more accentuated for the

samples HP2 and HP3 showing approximately similar or slightly less strength than HP1 after exposure.

Table 4. Compressive strength test results and standard deviations.

		COMPRESSIVE STRENGTH		
Temperature	Reference	HP1	HP2	HP3
25	4.17 ± 2.74	24.25 ± 2.374	31.68 ± 1.953	33.21 ± 1.402
500		22.377 ± 0.729	22.779 ± 1.578	23.108 ± 0.105
800		19.264 ± 2.099	18.433 ± 1.399	20.248 ± 0.551
1000		21.434 ± 2.059	17.999 ± 0.207	18.730 ±0.626

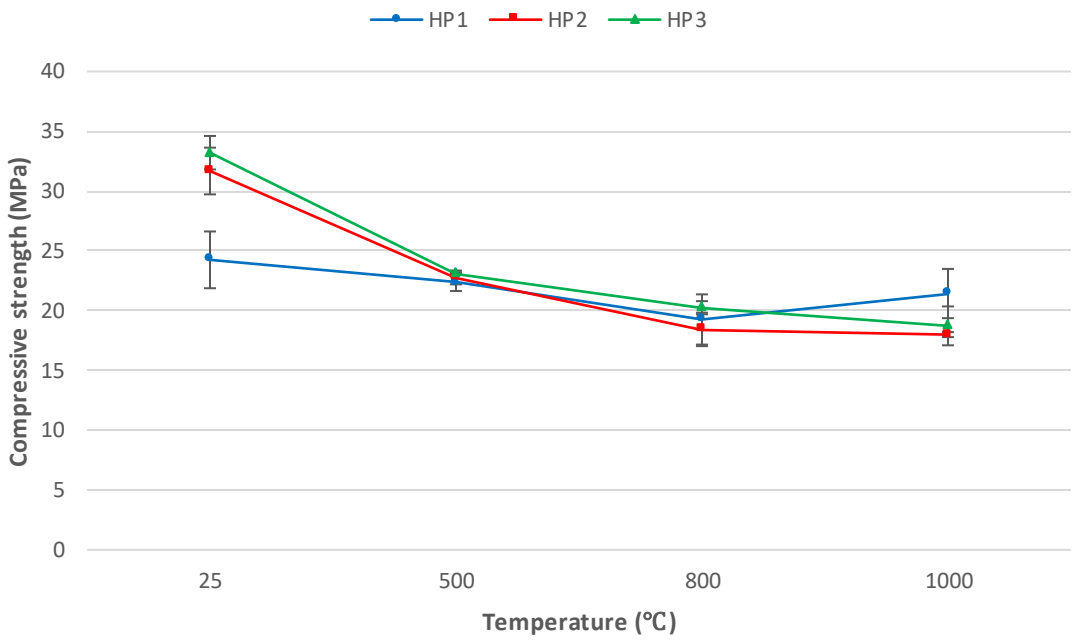

Figure 9. Compressive strength as a function of heating temperature. Error bars represent standard deviations of each result.

Ye et al. (2014) studied the effect of elevated temperature on the properties of geopolymer. The results showed that the samples underwent a shrinkage after exposure to high temperatures up to 700 °C and an expansion took place between 700 and 800 °C. A free water loss and gel dehydration were observed to cause the shrinkage whereas the

expansion was resulting from a volume increase due to the phase transition of the quartz. Simultaneously, the compressive strength of the samples decreased while exposing the samples to 1000 °C due to the increasing cracks and porosity caused by dehydration, dehydroxylation, and thermal incompatibility between forming geopolymer gel and expanding quartz. Also, Zhang et al. (2016) observed that the strength decrease of the geopolymer samples was caused by dehydration and dehydroxylation, as well as thermal incompatibility between the geopolymer paste and aggregates.

After exposure to 1200 °C, the samples gained strength caused by the viscous sintering and the formation of ceramic phases (Ye et al., 2014). Mustafa Al Bakri et al. (2013) observed similar changes in their microstructure study of FA-based geopolymer at elevated heat treatment temperature. A sintering process took place for unreacted FA microspheres while the samples were exposed to high temperatures. The sintering process was most effective after exposing the samples to 800 °C. In a study conducted by Moukannaa et al. (2019) the fusion of unreacted particles and the reformation of the geopolymer paste was also observed at 800 °C causing a strength gain in mortar samples.

Leaning on the studies above, the compressive strength loss of HP1, HP2, and HP3 in this thesis is probably caused by chemical reactions happening in high temperatures which lead to water loss and more porous structure in samples. Only HP1 gains strength between 800 and 1000 °C, which indicates to completion of alkali activation reaction for unreacted particles or fusion of mineral phases, which both fill the pores making the gel structure denser. It seems that the hot-pressing temperature affects the thermal stability of PPFA-based AAMs. HP1 retains its compressive strength during the thermal treatment better than HP2 and HP3. Comparing the graphs in Figure 7 and figure 8 it can be observed that the temperature-induced degradation is higher in flexural strength than in compressive strength. It is because flexural strength is more sensitive to internal structural defects, especially microcracks, caused by high temperatures than compressive strength (Zhang et al., 2016).

5 CONCLUSIONS

In this study, a hot-pressing technique was used to prepare three sets of PMA-based alkali-activated samples. A set of reference samples were also prepared using the conventional curing method at 60 °C. The samples were treated at a high-temperature oven and their mechanical properties including compressive and flexural strengths were measured before and after the heat treatments. Additionally, an XRD analysis was made to observe the samples' mineralogical changes and phase transitions.

The results showed that the hot pressing is very useful compared to the conventional curing method. It increased the mechanical properties of the samples by accelerating the alkali-activation reaction and making the gel structure denser. Flexural strength was 0.89 MPa for the samples cured at 60 °C while an average value for hot-pressed samples was 7.59 MPa. Compressive strength was 4.17 MPa and 29.71 MPa, respectively. The XRD results showed the formation of amorphous content which generally leads to better mechanical properties in AAMs. The compressive and flexural strength test results revealed good thermal resistance to hot-pressed samples. For all the samples, compressive strength retained its value near to 20 MPa even after being exposed to 1000 °C. The best thermal resistance was measured for HP1, which even gained compressive strength between 800 °C and 1000 °C. It indicates the completion of the alkali-activation reaction.

Hot-pressed PMA needs to be further studied in the future to investigate the durability and sustainability aspects. More than two average results in mechanical test calculations could be used to get more accurate results. Scanning electron microscopy (SEM) could also be performed to get more information about the changes in samples before and after the thermal treatments.

REFERENCES

Amran, Y. M., Alyousef, R., Alabduljabbar, H., & El-Zeadani, M. (2020). Clean production and properties of geopolymer concrete; A review. *journal of cleaner production*, *251*, 119679.

Barbosa, V. F., & MacKenzie, K. J. (2003). Thermal behavior of inorganic geopolymers and composites derived from sodium polysialate. *Materials research bulletin*, *38*(2), 319-331.

Cherian, C., & Siddiqua, S. (2019). Pulp and paper mill fly ash: A review. *Sustainability*, *11*(16), 4394.

Cristelo, N., Tavares, P., Lucas, E., Miranda, T., & Oliveira, D. (2016). Quantitative and qualitative assessment of the amorphous phase of a Class F fly ash dissolved during alkali activation reactions–Effect of mechanical activation, solution concentration, and temperature. *Composites Part B: Engineering*, *103*, 1-14.

Environment, U. N., Scrivener, K. L., John, V. M., & Gartner, E. M. (2018). Eco-efficient cements: Potential economically viable solutions for a low-CO2 cement-based materials industry. *Cement and Concrete Research*, *114*, 2-26.

Epp, J. (2016). X-ray diffraction (XRD) techniques for materials characterization. In *Materials characterization using nondestructive evaluation (NDE) methods* (pp. 81-124). Woodhead Publishing

Fan, F., Liu, Z., Xu, G., Peng, H., & Cai, C. S. (2018). Mechanical and thermal properties of fly ash-based geopolymers. *Construction and Building Materials*, *160*, 66-81.

Firdous, R., Hirsch, T., Klimm, D., Lothenbach, B., & Stephan, D. (2021). Reaction of calcium carbonate minerals in sodium silicate solution and its role in alkali-activated systems. *Minerals Engineering*, *165*, 106849.

Firdous, R., & Stephan, D. (2021). Impact of the mineralogical composition of natural pozzolan on properties of resultant geopolymers. *Journal of Sustainable Cement-Based Materials*, *10*(3), 149-164.

Zhang, H. Y., Kodur, V., Wu, B., Cao, L., & Qi, S. L. (2016). Comparative thermal and mechanical performance of geopolymers derived from metakaolin and fly ash. *Journal of Materials in Civil Engineering*, *28*(2), 04015092.

Zhang, H. Y., Kodur, V., Wu, B., Cao, L., & Wang, F. (2016). Thermal behavior and mechanical properties of geopolymer mortar after exposure to elevated temperatures. *Construction and Building Materials*, *109*, 17-24.

Hackett, G. A., Easton, C. A., & Duff, S. J. (1999). Composting of pulp and paper mill fly ash with wastewater treatment sludge. *Bioresource Technology*, *70*(3), 217-224

Hassan, A., Arif, M., & Shariq, M. (2019). Use of geopolymer concrete for a cleaner and sustainable environment–A review of mechanical properties and microstructure. *Journal of cleaner production*, *223*, 704-728.

He, R., Dai, N., & Wang, Z. (2020). Thermal and mechanical properties of geopolymers exposed to high temperature: a literature review. *Advances in Civil Engineering*, *2020*.

Kong, D. L., Sanjayan, J. G., & Sagoe-Crentsil, K. (2007). Comparative performance of geopolymers made with metakaolin and fly ash after exposure to elevated temperatures. *Cement and concrete research*, *37*(12), 1583-1589.

Mangat, P., & Lambert, P. (2016). Sustainability of alkali-activated cementitious materials and geopolymers. In *Sustainability of construction materials* (pp. 459-476). Woodhead Publishing.

Mehmet, K. A. Y. A., Uysal, M., Yilmaz, K., & Atis, C. D. (2018). Behaviour of geopolymer mortars after exposure to elevated temperatures. *Materials Science*, *24*(4), 428-436.

Mohammed, B. S., & Fang, O. C. (2011). Mechanical and durability properties of concretes containing paper-mill residuals and fly ash. *Construction and Building Materials*, *25*(2), 717-725

Moukannaa, S., Nazari, A., Bagheri, A., Loutou, M., Sanjayan, J. G., & Hakkou, R. (2019). Alkaline fused phosphate mine tailings for geopolymer mortar synthesis: Thermal stability, mechanical and microstructural properties. *Journal of Non-Crystalline Solids*, *511*, 76-85

Mustafa Al Bakri, A. M., Abdulkareem, O. A., Kamarudin, H., Khairul Nizar, I., Rafiza, A. R., Zarina, Y., & Alida, A. (2013). Microstructure studies on the effect of the alkaline activators of fly ash-based geopolymer at elevated heat treatment temperature. In *Applied Mechanics and Materials* (Vol. 421, pp. 342-348). Trans Tech Publications Ltd.

Pacheco-Torgal, F., Castro-Gomes, J., & Jalali, S. (2008). Alkali-activated binders: A review: Part 1. Historical background, terminology, reaction mechanisms, and hydration products. *Construction and Building Materials*, *22*(7), 1305-1314.

Pacheco-Torgal, F., Castro-Gomes, J., & Jalali, S. (2008). Alkali-activated binders: A review. Part 2. About materials and binders manufacture. *Construction and Building Materials*, *22*(7), 1315-1322.

Palomo, A., Grutzeck, M. W., & Blanco, M. T. (1999). Alkali-activated fly ashes: A cement for the future. *Cement and concrete research*, *29*(8), 1323-1329.

Provis, J. L., & Van Deventer, J. S. (Eds.). (2013). *Alkali activated materials: state-of-the-art report, RILEM TC 224-AAM*(Vol. 13). Springer Science & Business Media.

Rajamma, R., Ball, R. J., Tarelho, L. A., Allen, G. C., Labrincha, J. A., & Ferreira, V. M. (2009). Characterization and use of biomass fly ash in cement-based materials. *Journal of hazardous materials*, *172*(2-3), 1049-1060.

Ranjbar, N., Kashefi, A., & Maheri, M. R. (2018). Hot-pressed geopolymer: Dual effects of heat and curing time. *Cement and Concrete Composites*, *86*, 1-8.

Ranjbar, N., Kashefi, A., Ye, G., & Mehrali, M. (2020). Effects of heat and pressure on hot-pressed geopolymer. *Construction and Building Materials*, *231*, 117106.

Ranjbar, N., Mehrali, M., Maheri, M. R., & Mehrali, M. (2017). Hot-pressed geopolymer. *Cement and Concrete Research*, *100*, 14-22.

Sarkar, R., Kurar, R., Gupta, A. K., Mudgal, A., & Gupta, V. (2017). Use of paper mill waste for brick making. *Cogent Engineering*, *4*(1), 1405768.

Singh, N. B., Kumar, M., & Rai, S. (2020). Geopolymer cement and concrete: Properties. *Materials Today: Proceedings*, *29*, 743-748.

Singh, N. B., & Middendorf, B. (2020). Geopolymers as an alternative to Portland cement: An overview. *Construction and Building Materials*, *237*, 117455.

Wardhono, A. (2018). Comparison study of class F and class C fly ashes as cement replacement material on strength development of non-cement mortar. In *IOP Conference Series: Materials Science and Engineering* (Vol. 288, No. 1, p. 012019). IOP Publishing.

Ye, J., Zhang, W., & Shi, D. (2014). Effect of elevated temperature on the properties of geopolymer synthesized from calcined ore-dressing tailing of bauxite and ground-granulated blast furnace slag. *Construction and Building Materials*, *69*, 41-48

Zhang, H. Y., Kodur, V., Qi, S. L., Cao, L., & Wu, B. (2014). Development of metakaolin–fly ash-based geopolymers for fire resistance applications. *Construction and Building Materials*, *55*, 38-45.

Zhuang, X. Y., Chen, L., Komarneni, S., Zhou, C. H., Tong, D. S., Yang, H. M., ... & Wang, H. (2016). Fly ash-based geopolymer: clean production, properties, and applications. *Journal of Cleaner Production*, *125*, 253-267.